Time Modulated Array Controlled by Periodic Pulsed Signals

Roberto Maneiro-Catoira, Julio Brégains, José A. García-Naya, and Luis Castedo
University of A Coruña, Department of Computer Engineering, A Coruña, Spain.
E-mail:{roberto.maneiro, julio.bregains, jagarcia, luis}@udc.es

***Abstract*—During the last years, time-modulated array (TMA) architectures have been considering different switching network designs, focusing primarily on the radiation pattern synthesis. Unfortunately, switching networks exhibit a noticeable energy leakage due to the time the array elements remain off, yielding a strong degradation of the signal-to-noise ratio. To improve the corresponding network efficiency, configurations with multiple switches per antenna element, or even with single-pole multiple-throw switches, have been proposed. However, network switching efficiency improvements sacrifice beamforming flexibility. To overcome such a limitation, recent works have proposed to replace the switches with variable-gain amplifiers controlled by time-variant pulses based exclusively on sinusoids. In this work, we describe a TMA architecture based on ultra-wide band analog multipliers which is suitable for all kind of periodic pulses.**

***Index Terms*—Antenna arrays, time-modulated arrays, beamforming.**

I. Introduction

Early time-modulated array (TMA) schemes considered the simplest possible architecture, consisting of one single-pole single-throw (SPST) switch per antenna element plus a summing circuit, whereas the TMA design focused exclusively on the radiation pattern synthesis [1]. However, key aspects such as the energy inefficiency caused by the waste of power when the switches are disconnected, or the reduction of the average signal-to-noise ratio (SNR) at the receiver, were not considered until TMAs were proposed for multiple beamforming in communications [2]. In such circumstances, single-pole multiple-throw (SPMT) switches have been explored to overcome the enormous gain degradation per beam of the radiation pattern. Nevertheless, the use of a single radio frequency (RF) switch for controlling multiple antenna elements implies a TMA design with complementary switch-on time durations, leading to a less flexible beamforming, which is impractical for more than two harmonic beams. TMA schemes using single-pole dual-throw (SPDT) switches have been proposed in [3] to improve the TMA beamforming efficiency. Such techniques are based on preprocessing the TMA pulses in a way that resembles single sideband (SSB) modulation, hence the name SSB TMA to refer to such techniques. SSB TMAs, however, are limited to beamforming the first positive harmonic. In order to circumvent those limitations, other solutions have been proposed in the literature, which led to, for example, the design of multibeam TMAs based on the use of alternative periodic pulsed signals such as sum of weighted cosines (SWC) [4], or digitally preprocessed rectangular pulses [5].

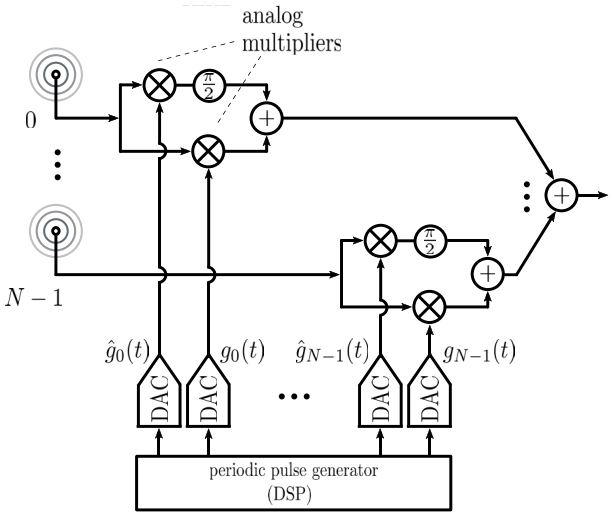

Fig. 1. Proposed TMA architecture with analog multipliers to perform the periodic pulse modulation.

Time modulation with such alternative periodic pulsed signals is implemented with variable-gain amplifiers (VGAs) rather than switches, making possible a more flexible multiple beamforming. Inspired in the latter schemes, we propose in this work a more generic concept: a TMA structure that can be controlled by any kind of periodic pulsed signal, employing analog multipliers to perform the periodic pulse modulation. We believe that this is the first work that proposes such a TMA structure supporting multiple beamforming at the fundamental and harmonic frequencies.

II. Mathematical Fundamentals

Let us consider a linear array with N isotropic elements with unitary complex static excitations $I_n = 1$, $n \in \{0, 1, \ldots, N-1\}$. As shown in Fig. 1, each element excitation is modulated by a pair of periodic pulsed signals: $\mathrm{g}_n(t)$ and its Hilbert Transform (HT) $\hat{g}_n(t)$, both with the fundamental period T_0. Such periodic signals are generated in the digital domain, and then converted to the continuous-time domain through the corresponding digital-to-analog converters (DACs). Fig. 1 also shows how the periodic pulse modulation is carried out by analog multipliers. Since $g_n(t) \in \mathbb{R}$, it can

ISBN 978-90-827970-1-5

be represented by the following trigonometric Fourier series:

$$g_n(t) = A_{n0} + 2\sum_{q=1}^{\infty} A_{nq}\cos(q\omega_o t + \Phi_{nq}), \quad (1)$$

being $\omega_0 = 2\pi/T_0$ and $a_{nq} = A_{nq}e^{j\Phi_{nq}} \in \mathbb{C}$ the exponential Fourier series coefficients of $g_n(t)$. As the $g_n(t)$ are real-valued, such coefficients satisfy $a_{n(-q)} = a_{nq}^*$ and hence $a_{n0} = A_{n0} \in \mathbb{R}$, which is its direct current (DC) component. Notice that

$$\hat{g}_n(t) = 2\sum_{q=1}^{\infty} A_{nq}\sin(q\omega_o t + \Phi_{nq}) \quad (2)$$

because the HT acts as a $\pi/2$ phase shifter of a given signal and setting to zero its DC component.

Let us next consider that a narrowband passband signal $u(t)e^{j\omega_c t}$ impinges on the array. The analytical representation of the incoming signal is given by $u(t)e^{j\omega_c t}$, where $u(t)$ is its complex-valued baseband equivalent. According to Fig. 1, the signal at the array output[1] will be

$$s(t,\theta) = u(t)e^{j\omega_c t}\sum_{n=0}^{N-1}(g_n(t) + j\hat{g}_n(t))e^{jkz_n\cos\theta}, \quad (3)$$

where z_n represents the n-th array element position on the z axis, θ is the angle with respect to such a main axis, and k is the wavenumber. By considering the Fourier Transforms (FTs) of Eq. (1) and that of its HT, we have that the FT of $s(t,\theta)$ is

$$S(\omega,\theta) = \frac{U(\omega-\omega_c)}{2\pi} * \sum_{n=0}^{N-1}\Big[A_{n0}\delta(\omega) + \\ + 2\sum_{q=1}^{\infty} A_{nq}\delta(\omega - q\omega_o)e^{j\Phi_{nq}}\Big]e^{jkz_n\cos\theta}, \quad (4)$$

being $*$ the convolution operator, $\delta(\omega)$ the unit impulse in the frequency domain, and $U(\omega)$ the FT of $u(t)$. It is important to note that the negative spectral lines are canceled out in the previous calculation. Turning back to the time domain, we arrive at

$$s(t,\theta) = 2u(t)\Big[F_{\omega_c}(\theta)e^{j\omega_c t} + \sum_{q=1}^{\infty} F_{\omega_c+q\omega_0}(\theta)e^{j(\omega_c+q\omega_0)t}\Big], \quad (5)$$

where

$$F_{\omega_c}(\theta) = \sum_{n=0}^{N-1} A_{n0}e^{jkz_n\cos\theta}, \text{ and}$$

$$F_{(\omega_c+q\omega_0)}(\theta) = \sum_{n=0}^{N-1} 2A_{nq}e^{j\Phi_{nq}}e^{jkz_n\cos\theta} \quad (6)$$

are the spatial array factors at frequencies ω_c and $\omega_c + q\omega_0$, respectively. Notice that the array factor at the fundamental frequency ω_c depends on the real-valued numbers A_{n0} and thus has no scanning ability, whereas the array factors at the harmonic frequencies $\omega_c + q\omega_0$ ($q \geq 1$) depend on the complex-valued coefficients $A_{nq}e^{j\Phi_{nq}}$ and therefore can be satisfactorily used to perform adaptive beamforming.

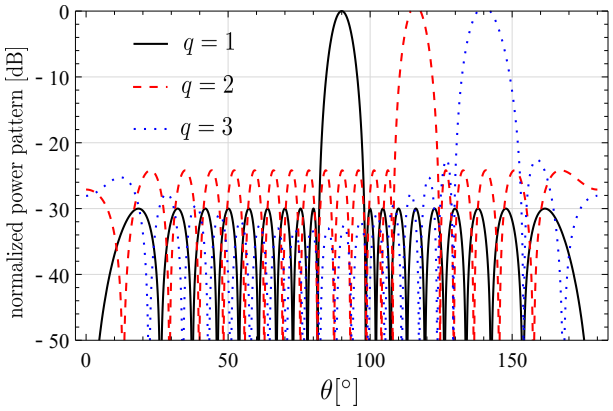

Fig. 2. The TMA in Fig. 1 can be used to synthesize three independently steerable radiation patterns (Dolph-Chebyshev with -30 and -25 dB of SLL, and a normalized Gaussian pattern with a standard deviation of $2/3$, respectively) over three different harmonics ($q = \{1,2,3\}$), and employing amplitude tapering supported by pure sinusoids.

III. Beamforming Configurations

In the following subsections we illustrate how the proposed TMA architecture shown in Fig. 1 is capable of supporting multiple beamforming at the fundamental and harmonic frequencies. We show that this is possible by employing suitable periodic pulsed signals and using amplitude and/or time tapering.

A. Pure Sinusoids (Amplitude Tapering)

By considering Eq. (1) with a finite sum of L pure sinusoids, and setting $A_{n0} = 0$, we have

$$g_n(t) = 2\sum_{q=1}^{L} A_{nq}\cos(q\omega_o t + \Phi_{nq}). \quad (7)$$

Under these premises, we can carry out the beamforming over $\omega_c + q\omega_0$ ($q \neq 0$) by controlling the amplitudes A_{nq} and the phases Φ_{nq} in the array factor $F_{\omega_c+q\omega_0}(\theta)$ given by Eq. (6). By considering $\Phi_{nq} = -q\omega_0\delta_{nq}$, being δ_{nq} a time delay, it is possible to easily implement L beamforming radiation patterns by controlling the amplitude tapering A_{nq} and the cosine time-delays δ_{nq}. Recall that the harmonic radiation patterns can be totally independent in amplitude and phase. As a matter of fact, we have considered the example in Fig. 2, which corresponds to an array of $N = 20$ elements exploiting $L = 3$ harmonics. $\{A_{n1}\}$, $\{A_{n2}\}$, and $\{A_{n3}\}$ are selected as the normalized amplitude excitations corresponding to a Dolph-Chebyshev distribution with -30 dB of SLL, a Dolph-Chebyshev distribution with -25 dB of SLL, and a Gaussian pattern with a standard deviation of $2/3$, respectively. For each q, δ_{nq} are progressive phases so that the corresponding

[1]Notice that if B is the signal bandwidth, then $\omega_o > B$ [2] and the sampling frequency of the DACs, ω_s, must satisfy $\omega_s > 2L\omega_0$, being L the order of the highest harmonic to be exploited.

ISBN 978-90-827970-1-5

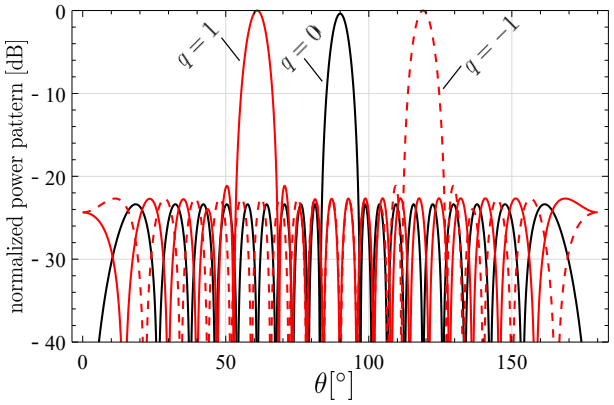

Fig. 3. Radiation pattern [4, Fig. 10] synthesized by means of an architecture based on VGAs known as Enhanced TMA. The application of identical 2-term ($K = 1$) SWC pulses with $a_{n0} = 1/3$, $a_{n1} = 2/3$, and normalized time durations ξ_n capable of synthesizing Dolph-Chebyshev pencil beam patterns with SLL $= -23$ dB, generates the beams in the figure at $q = 0$, $q = 1$ and $q = -1$, respectively. In this work, thanks to the structure in Fig. 1, where both $g_n(t)$ and $\hat{g}_n(t)$ are applied to the antenna, we improve the beamforming efficiency by removing the specular beam at $q = -1$ (symmetric to the one for $q = 1$ with respect to $\theta = 90°$).

beams point to 90°, 116°, and 140°, respectively. Notice also that the proposed architecture allows for improving the antenna efficiency when compared to [6] because it removes the specular patterns corresponding to the negative harmonics.

B. SWC Pulses (Amplitude & Time Tapering)

The so-called Enhanced TMAs [4] based on SWC pulses can perform both amplitude and time control of the array excitations. According to this technique, each periodic pulsed signal, $g_n(t)$, is obtained after the following two steps:

1) We first construct the periodic (T_0) extension of a basic (aperiodic) pulse given by an SWC over a finite duration $\tau_n \leq T_0$, i.e.,

$$b_n(t) = \sum_{k=0}^{K} a_{nk} \cos(2\pi k t/\tau_n)\, \mathrm{rect}(t/\tau_n), \qquad (8)$$

where $\mathrm{rect}(t/\tau_n) = 1$ for $t \in (-\tau_n/2, \tau_n/2)$, and 0 otherwise; and a_{nk} are real-valued constants with $k \in \{0, 1, \ldots, K\}$ satisfying the normalization condition $\sum_{k=0}^{K} a_{nk} = 1$. The functions given in Eq. (8) have been used to design different windowing functions with excellent sidelobe behavior [7]. The Fourier coefficients of the periodic pulse train with $b_n(t)$ as in Eq. (8) are [4]

$$B_{nq} = \frac{\xi_n^2 q}{\pi} \sin(\pi \xi_n q) \sum_{k=0}^{K} \frac{(-1)^k a_{nk}}{\xi_n^2 q^2 - k^2}, \qquad (9)$$

being $\xi_n = \tau_n/T_0$ the normalized pulse durations.

2) We next obtain $g_n(t)$ by time-shifting δ_n the previous periodic pulsed signal. The resulting periodic signal will have Fourier series coefficients given by $B_{nq} \mathrm{e}^{-jq2\pi/T_0\delta_n}$ and, therefore, it is immediate that A_{nq} and Φ_{nq} in Eq. (1) will satisfy

$$A_{nq} = \frac{\xi_n^2 q}{\pi} \sin(\pi \xi_n q) \sum_{k=0}^{K} \frac{(-1)^k a_{kn}}{\xi_n^2 q^2 - k^2}, \text{ and}$$
$$\Phi_{nq} = -q\omega_0 \delta_n. \qquad (10)$$

In view of Eq. (10), the designer has two degrees of freedom (time durations ξ_n and cosine weights a_{nk}) in the expression of A_{nq}. Notice that $\Phi_{n1} = -\omega_0 \delta_n$ are the phases of the excitations of the first-order harmonic. Therefore, the phases for a given higher-order harmonic q will be $\Phi_{nq} = q\Phi_{n1}$, hence showing proportional phases that may limit the beamforming design when the number of harmonics increases. In order to synthesize harmonic beams with independent phases, the periodic convolution of SWC pulse trains with auxiliary pure cosine signals is proposed in [4].

Fig. 3 illustrates how the proposed architecture improves the beamforming efficiency exhibited by an Enhanced TMA synthesizing the same radiation pattern but removing the specular ($q = -1$) beam.

C. Nyquist Pulses (Accurate Harmonic Windowing)

Focusing again on TMA harmonic beamforming, it is well-known that the frequency behavior of conventional rectangular pulses, implemented by RF switches, is not the best one to efficiently distribute the spectral energy among the different harmonic patterns to be exploited [4], especially when more than a single harmonic radiation pattern is to be synthesized. A minimum main-lobe width and a modest SLL, together with a slow asymptotic side-lobe decay—quantitatively reflected in $A_{nq} = \tau_n/T_0 \mathrm{sinc}(q\pi\tau_n/T_0)$, see Fig. 4 (a)—are characteristics of the rectangular pulse frequency response which will restrict the TMA efficiency together with the SNR at the receiver.

The versatility of the proposed structure shown in Fig. 1 allows for considering periodic Nyquist pulsed signals. Notice that such periodic pulsed signals are the most suitable (and long-established) alternative to the non-causal ideal sinc function with an infinite time response.

Let us consider the well-known Nyquist pulse [8]

$$r(t) = \mathrm{sinc}(2\pi t/\tau_n) \cos \frac{2\rho_n \pi t/\tau_n}{1 - (4\rho_n t/\tau_n)^2}, \qquad (11)$$

where τ_n is the duration between zero crossings (see Fig. 4 (b)) and $\rho_n \in [0, 1]$ is the roll-off factor, which determines the smoothness of the pulse frequency response. We can construct $g_n(t)$ given by Eq. (1) as the periodic extension of $r(t)$, being T_0 large enough with respect to τ_n. Fig. 4 (b) shows the magnitude of such a periodic pulse which, additionally, can be shifted in time δ_n with respect to $t = 0$. Then, the FT of $g_n(t)$ will be (see Fig. 4 (b)) [8], a frequency comb at $\omega = q\omega_0$ ($q \in \mathbb{Z}$), whose envelope is

ISBN 978-90-827970-1-5

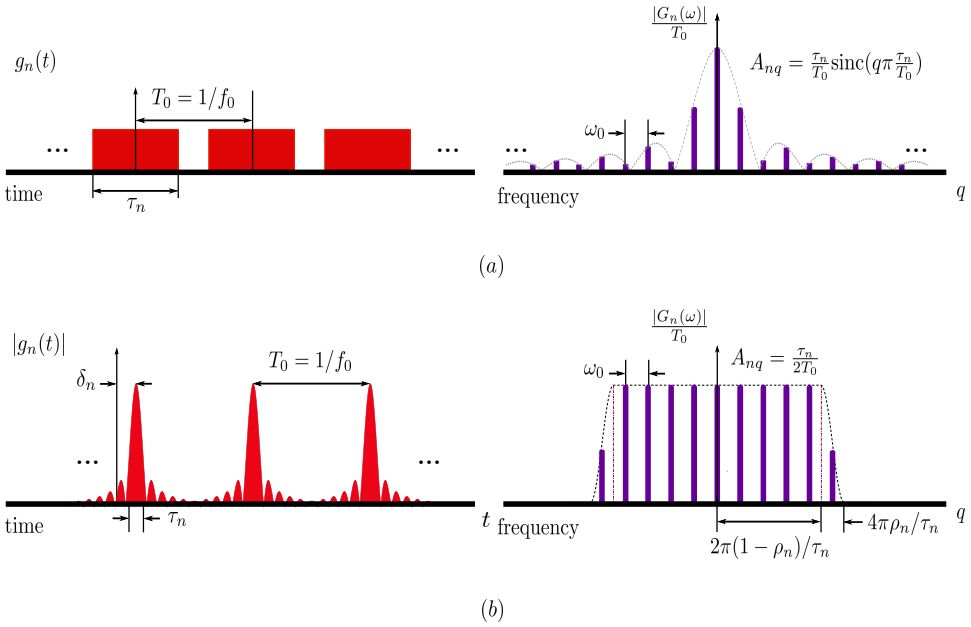

Fig. 4. (a) Periodic rectangular pulsed signal and its frequency response showing poor harmonic windowing characteristics, evidenced by the corresponding A_{nq} expression. (b) The versatility of the proposed structure shown Fig. 1 allows for generating a periodic train of Nyquist pulses with a duration τ_n between zero crossings and a roll-off factor ρ_n. The spectral lines—with magnitude A_{nq}—are under a practically rectangular windowing envelope corresponding to a raised-cosine envelope.

$$G_n(\omega) = \begin{cases} \tau_n/2 & |\omega| < \omega_1 \\ \dfrac{\tau_n}{4}\left[1 + \cos\left(\dfrac{\pi(|\omega| - \omega_1)}{2\pi/\tau_n - 2\omega_1}\right)\right] & \omega_1 \le |\omega| \le \omega_2 \\ 0 & |\omega| > \omega_2, \end{cases} \tag{12}$$

being $\omega_1 = 2\pi(1-\rho_n)/\tau_n$ and $\omega_2 = 2\pi(1+\rho_n)/\tau_n$. Hence, the Fourier series coefficients in Eq. (1) for $q < \omega_1/\omega_0$ will be $a_{nq} = G_n(q\omega_0)/T_0 = \tau_n/(2T_0)\text{e}^{-jq\omega_0\delta_n}$. Therefore, if we want to fix the order (L) of the identical harmonic patterns to be exploited (flat response of $G_n(\omega)$), we can keep constant the bandwidth $2\omega_1$ (see Fig. 4 (b)), i.e.,

$$2\pi(1-\rho_n)/\tau_n = L\omega_0, \tag{13}$$

leading to $\tau_n = (1-\rho_n)T_0/L$. On the other hand, if we want to guarantee that the harmonic with order $L+1$ (and beyond) be totally suppressed, the following condition must be satisfied (see Fig. 4 (b)):

$$4\pi\rho_n/\tau_n < 2\pi/T_0, \tag{14}$$

thus arriving at the condition $\rho_n < \tau_n/(2T_0)$ for the selection of ρ_n. Under these assumptions, we have that A_{nq} and Φ_{nq} in Eq. (1) are given by

$$\begin{aligned} A_{nq} &= \tau_n/(2T_0), \text{ and} \\ \Phi_{nq} &= -q\omega_0\delta_n. \end{aligned} \tag{15}$$

Finally, we next show two examples of application of the scheme proposed in Fig. 1 when controlled by periodic Nyquist pulses.

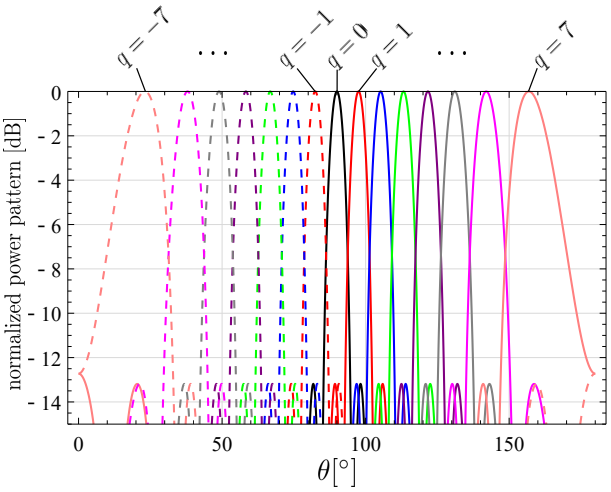

Fig. 5. Radiation pattern of the proposed structure controlled by Nyquist pulses. For this application we have considered $\hat{g}_n(t)$=0 in order to intentionally generate negative and positive harmonic patterns to efficiently perform direction finding using 15 simultaneous beams.

1) Direction Finding: The proposed TMA governed by Nyquist pulses has the capacity of generating a reconfigurable number of identical uniform steerable harmonic beams. Hence, it can be applied to compare the strength of simultaneously received signals (over the different harmonic beams pointing towards different directions) in order to determine the direction of arrival (DOA) of a desired signal. Fig. 5 illustrates an example of radiation pattern using 15 beams where the complex structure of the array is not exploited deliberately (i.e., $\hat{g}_n(t) = 0$) with the aim of generating also the negative

ISBN 978-90-827970-1-5

patterns in order to cover as much spatial directions as possible in a simple way.

2) Multipath Receiver: The proposed system is capable of exploiting the harmonic patterns at reception by transforming spatial diversity into frequency diversity. By means of a receiver scheme equipped with a maximum ratio combining (MRC) as the one shown in [2, Fig. 1]—considering the proposed TMA shown in Fig. 1 instead of that in [2, Fig. 1]—it is possible to design a wireless communication receiver capable of profitably exploiting channel diversity in the form of angular diversity captured by the sideband radiation (harmonic patterns) exhibited by the TMA. Once again, the differentiating advantage of this system is its SSB ability that improves the antenna efficiency as well as the SNR. Notice that the main behavior difference of this scheme based on Nyquist pulses with respect to conventional TMAs is that the normalized pulse durations in the time domain, ξ_n, are employed solely to determine the number of harmonics to be exploited, whereas the pulse time-shifts δ_n are set to point towards the different incoming signals. Hence, by fixing the same ξ_n for all n we will synthesize $L+1$ uniform radiation patterns over the corresponding frequencies $\omega_c + q\omega_0$ with $q = 0, 1, \ldots, L$. Fig. 6 shows a radiation pattern for $L = 3$. The limitations of the proposed technique for this application is the synthesis (exclusively) of uniform patterns with an SLL of -13 dB and the non-steerable pattern at $q = 0$.

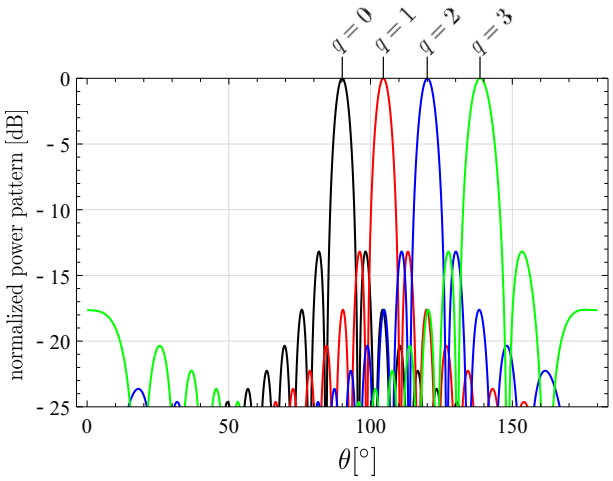

Fig. 6. Radiation pattern example obtained with the proposed TMA structure controlled with Nyquist pulses and applied to a multipath reception considering $L+1=4$ multipath components (signal replicas). Notice that the beam for $q=0$ is not endowed with steering ability (as usual in TMAs).

IV. Conclusions

We have proposed a novel TMA architecture supporting multiple beamforming at the fundamental and harmonic frequencies that is controlled by generic periodic pulses using amplitude and/or time tapering. We have modeled mathematically the radiation features of the proposed TMA architecture and have shown its applicability by analyzing its behavior with a varied range of periodic signals. We have also explored potential applications such as signal direction finding or spatial diversity exploitation with a multipath receiver that converts it into frequency diversity, thus requiring a single RF branch—with larger bandwidth— to receive all the signal replicas.

Acknowledgment

This work has been funded by the Xunta de Galicia (ED431C 2016-045, ED341D R2016/012, ED431G/01), the Agencia Estatal de Investigacin of Spain (TEC2015-69648-REDC, TEC2016-75067-C4-1-R) and ERDF funds of the EU (AEI/FEDER, UE).

References

[1] L. Poli, P. , G. Oliveri, and A. Massa, "Harmonic beamforming in time-modulated linear arrays," *IEEE Transactions on Antennas and Propagation*, vol. 59, no. 7, pp. 2538–2545, July 2011.

[2] R. Maneiro Catoria, J. Brégains, J. A. Garcia-Naya, L. Castedo, P. Rocca, and L. Poli, "Performance analysis of time-modulated arrays for the angle diversity reception of digital linear modulated signals," *IEEE Journal of Selected Topics in Signal Processing*, vol. 11, no. 2, pp. 247–258, Mar. 2017.

[3] A. M. Yao, W. Wu, and D. G. Fang, "Single-sideband time-modulated phased array," *IEEE Transactions on Antennas and Propagation*, vol. 63, no. 5, pp. 1957–1968, May 2015.

[4] R. Maneiro Catoria, J. Brégains, J. A. Garcia-Naya, and L. Castedo, "Enhanced time-modulated arrays for harmonic beamforming," *IEEE Journal of Selected Topics in Signal Processing*, vol. 11, no. 2, pp. 259–270, Mar. 2017.

[5] R. Maneiro-Catoira, J. Brgains, J. A. Garca-Naya, and L. Castedo, "Frequency-domain synthesis of time-modulated arrays," in *Proc. of 2017 IEEE International Symposium on Antennas and Propagation USNC/URSI National Radio Science Meeting*, San Diego, California, USA, Jul. 2017, pp. 1041–1042.

[6] C. He, A. Cao, X. Liang, R. Jin, and J. Geng, "Beamforming method with periodical amplitude modulation array," in *Proc. of 2013 IEEE Antennas and Propagation Society International Symposium (APSURSI)*, Jul. 2013, pp. 874–875.

[7] A. H. Nuttall, "Some windows with very good sidelobe behavior," *Acoustics, Speech and Signal Processing, IEEE Transactions on*, vol. 29, no. 1, pp. 84–91, Feb 1981.

[8] A. Goldsmith, *Wireless Communications*. Cambridge University Press, 2005.